Direct Observation of Three-Dimensional Bicontinuous Structure Developed via Spinodal Decomposition

Hiroshi Jinnai,*,† Yukihiro Nishikawa,† Tsuyoshi Koga,† and Takeji Hashimoto†,‡

Hashimoto Polymer Phasing Project, ERATO, JRDC, Morimoto-cho, Shimogamo, Sakyo-ku, Kyoto 606, Japan, and Division of Polymer Chemistry, Graduate School of Engineering, Kyoto University, Kyoto 606-01, Japan

Received March 3, 1995

The dynamics and pattern formation in systems undergoing spinodal decomposition (SD) has been the subject of many theoretical and experimental investigations as a fascinating example of nonlinear, nonequilibrium phenomena.[1−3]

In order to study the phase separation process, two different types of analyses are used to characterize the structure: real-space analysis using microscopy[4] and reciprocal-space analysis using a variety of scattering methods such as light,[5] neutron,[6] and X-ray scattering.[7] The scattering methods are useful for studying the statistical properties of phase-separated structures (e.g., the characteristic wavelength of the dominant mode of the phase-separating structure can be evaluated[8] but do not offer an intuitive insight into the structures.

On the other hand, microscopy offers images of the phase-separated structures. Compared with the scattering method, it is often more intuitive but less quantitative because of the limited region of observation. A major difficulty with using a microscope to observe complex structures comes from the fact that the focal depth is often too thick for the structure. This is not the case if the structure gets large enough to be comparable in size with the thickness of the specimen, but in these circumstances the phase-separation process becomes necessarily influenced by its two-dimensional (2D) nature. Since we are interested in the phase-separated structures evolved in three-dimensional (3D) space, we would like to avoid this 2D effect as much as possible.

Laser scanning confocal microscopy (LSCM) avoids out-of-focus information from neighboring planes.[9] Light reflected from the specimen is focused through a small aperture (i.e., confocal pinhole), which ensures that information only arrives from a particular level of the specimen. Changing the position of the focal plane in the specimen by vertically moving either the specimen or the objective makes a series of optically sectioned images along the axis perpendicular to the focal plane, which can then be used to reconstruct a 3D image by computationally stacking the images. LSCM has been extensively used in the fields of biology and medical science to investigate cell structures.[10] A few applications to polymer mixtures have been made.

To our knowledge, Verhoogt et al.[11] first reported the application of LSCM to a polymeric mixture, in which they presented a 3D image of the structure of the blends. Although Verhoogt et al. compared their LSCM images with those from transmission electron microscopy and scanning electron microscopy, their report was instrument oriented and thus did not provide much insight into the phase-separated structure of the binary mixture itself. Li et al.[12] investigated the structure of a polystyrene (PS) and poly(methyl methacrylate) (PMMA) mixture by LSCM. They observed the discrete phase-separated morphology of the solvent-cast films of the mixture as a function of distance from the air−polymer surface.

The aim of the present study is to evaluate the quantities characterizing bicontinuous structures in bulk mixtures by LSCM, e.g., the mean curvature of the interface, which otherwise may be difficult to obtain from the conventional scattering methods.

A poly(styrene-*ran*-butadiene) (SBR)/polybutadiene (PB) mixture was used. The sample characteristics of the polymers are listed in Table 1. The blend has an upper critical solution temperature (UCST) type phase diagram.[13] SBR and PB were codissolved in toluene with 50/50 wt % composition and then cast into a film. The film specimen thus obtained was thoroughly dried in a vacuum oven at room temperature. The mixture was then homogenized by mechanical mixing using Baker's transformation[14] and placed between two coverslips. The assembly was annealed at 100 °C for about 2 days and subsequently observed by LSCM (Carl-Zeiss LSM410) at room temperature. Forty image slices (160 × 160 μm, 256 × 256 pixels), from 10 to 50 μm away from the coverslip with 1 μm increments, were taken with an oil-immersed ×40 objective.

Figure 1 shows a typical LSCM micrographic image of the SBR/PB mixture. Part a shows the raw image, while part b shows the corresponding binary image after image processing. Interfaces between adjacent coexisting domains appear as dark lines in the image. Although not shown in the present paper, the domains get thicker and the distance between the domains increases with time. A close look at the image shows that the domains consist of small white dots which we cannot identify at the moment. We note that the LSCM image looked dark-and-bright immediately after transferring the specimen from the hot plate at 100 °C to the sample stage of the microscope. However, as time elapsed, small white dots appeared in the black phase so that the image gradually lost contrast. This is probably due to the second temperature drop from 100 to 23 °C causing new phase separation in each domains. Although this produces some complications, the position of the interface between the domains definitely stayed unchanged over the time range of our observation.

We suspect that the contrast for reflection microscopy comes from the interface between the adjacent coexisting domains where the refractive index gradually changes. In the original dark-and-bright images, one of the domains contained small dotlike objects, which made the domains look bright. It is difficult, therefore, to identify whether the (initially) bright phase is an SBR-rich domain or a PB-rich domain. This problem could be solved by incorporating fluorescent molecules into one of the constituent polymers, and we are currently attaching anthracene to PB to enhance the contrast for LSCM.

Figure 2 shows the 3D image constructed from the confocal images. The white part of the figure represents one of the two domains, while the other domain is transparent and invisible. Figure 2 clearly demonstrates that the phase-separated structure is bicontinuous and interpenetrating. The white domain in the 3D representation is continuous over the space.

* To whom correspondence should be addressed.
† ERATO, JRDC.
‡ Kyoto University.

0024-9297/95/2228-4782$09.00/0

Table 1. Sample Characteristics

polymer	microstructure,[a] % 1,2	cis 1,4	trans 1,4	cont,[b] %	mol wt 10^4M_w[c]	10^4M_n[d]	M_w/M_n
SBR	17	31	52	20	17.9	14.8	1.2
PB	24	37	39		8.9	5.7	1.6

[a] Microstructure in the butadiene unit in SBR. Determined by infrared spectroscopy. [b] Weight percentage of styrene in SBR. Determined by ^{1}H-NMR. [c] Weight-average molecular weight. Determined by size-exclusion chromatography equipped with light scattering. [d] Number-average molecular weight. Determined by size-exclusion chromatography equipped with light scattering.

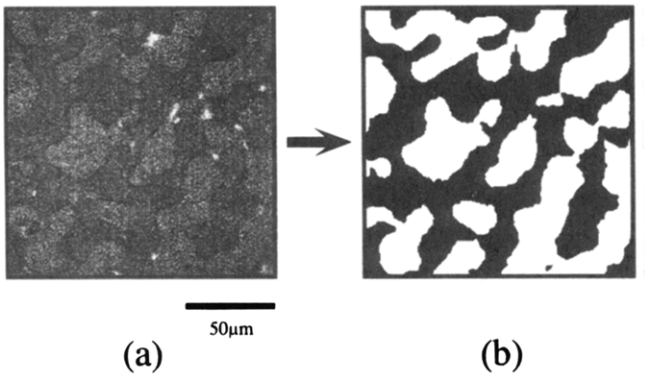

Figure 1. LSCM micrographic image of a SBR/PB mixture. (a) LSCM image at 10 μm from the coverslip. (b) Binary image of a after the image processing. The image is 160 × 160 μm in area (256 × 256 pixels). The black bar in the figure corresponds to 50 μm.

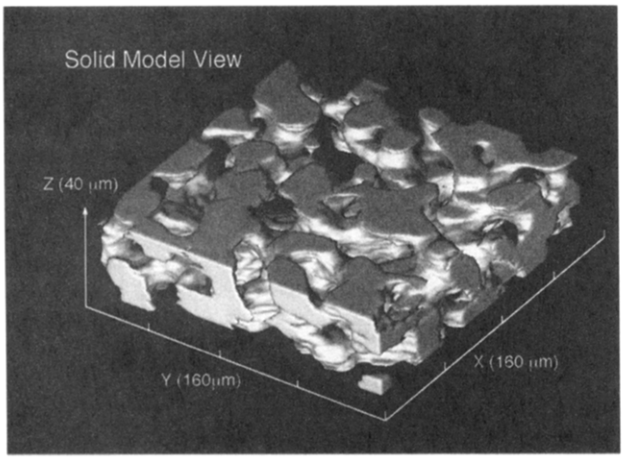

Figure 2. Solid modeling view of the SBR/PB phase-separating structure, reconstructed from 40 slices of image-processed LSCM pictures. A three-dimensional image-processing technique was used in order to reduce unnecessary noise from the original binary image. The optical sectioning width for the objective is approximately 1 μm, so no interpolation has been done in stacking the LSCM images.

For quantitative analysis, the structure factor $S(q)$ was obtained from the 3D image (Figure 2) by 3D Fourier transformation. $S(q)$ was then averaged in the q_x–q_y plane, where q_x and q_y denote respectively the x and y axes in Fourier space. In Figure 3, the $S(q)$ thus obtained is plotted double-logarithmically *vs* wavenumber, $q = 2\pi i/NL$ ($i = 0, 1, 2, ..., N/2$; $N = 256$), where L is the length of the pixels. The abscissa has been scaled by the wavelength, q_m, at maximum intensity and the column by the maximum intensity. The definition of q for the scattering experiment is given by $q = (4\pi/\lambda)\sin(\theta/2)$, where λ and θ are respectively the wavelength of the incident laser and the scattering angle.

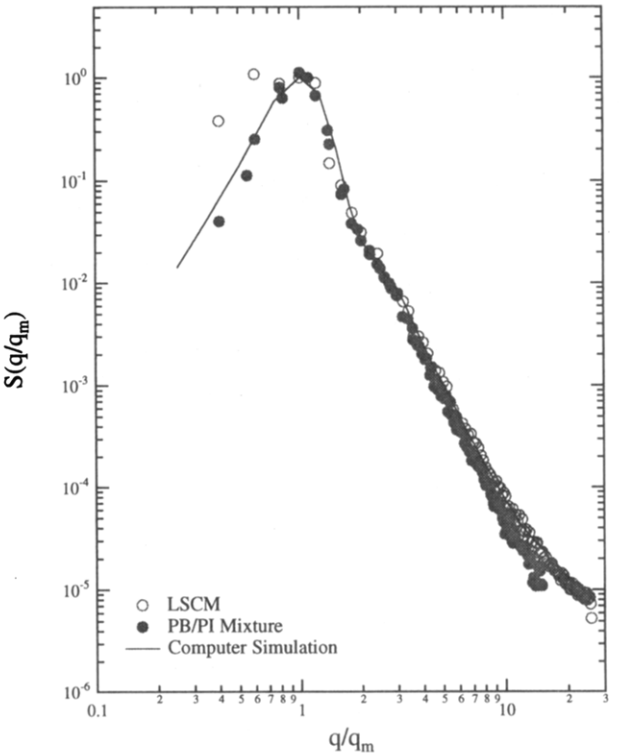

Figure 3. Structure factor $S(q/q_m)$ obtained by three different methods. The open circles represent the Fourier transformation of the LSCM image shown in Figure 2, and the filled circles represent the LS result from a PB/PI 50/50 wt % mixture. The solid line shows the result of a computer simulation using the TDGL equation.

$S(q)$ from the LSCM image (open circles) has q_m at 0.196 μm^{-1}. The characteristic wavelength, Λ_m, can be evaluated to be 32.1 μm according to the relationship $\Lambda_m = 2\pi/q_m$. We mention that the mixture should be well in the late stage of SD judging from the light scattering (LS) experiments on SBR/PB mixtures with different molecular weights.[15] It is worth noting that $S(q)$ has a weak shoulder-like second maximum at $q/q_m \cong 3$. This has been observed in several experiments[16] as well as computer simulations.[17,18] Bates et al.[19] reported a slightly different value, i.e., $q/q_m \cong 2$, that is inconsistent with this result. The essence of the problem is still unclear but may have something to do with the mean curvature of the phase-separated structure. The large scatter of $S(q)$ determined from the LSCM image in the small q region is due to the lack of statistical accuracy.

The filled circles in Figure 3 represent the LS result from the mixture of PB and polyisoprene (PI).[16] We should remark that $S(q/q_m)$ has been discussed for a SBR/PB mixture in the literature.[20] However, $S(q/q_m)$ in ref 19 was for a different composition, 40/60 wt %, from ours so the functional form may be different. Therefore, the $S(q)$ from PB/PI is the best one available for comparison at this moment. The solid line shows the result of a computer simulation in 3D space using the time-dependent Ginzburg–Landau equation in the hydrodynamic domain growth region.[18] That structure factor obtained from the LSCM image is in *excellent* and *quantitative* agreement with that from the other methods except for the data at $q/q_m > 5$.[21] This leads to the conclusion that the statistical nature of the phase-separated structure from the three different methods is identical. We note that all three structure factors were obtained in the late stage of SD.

In summary, the 3D image of a complex bicontinuous structure developed via spinodal decomposition (SD) was observed *in a real experimental system* by use of a laser scanning confocal microscope (LSCM). The Fourier transform of the image gave the structure factor, $S(q)$, which was compared with that from a scattering experiment in a polymeric mixture and with that from computer simulation. They agreed quantitatively, especially in terms of the existence of the higher order shoulder in $S(q)$. This clearly demonstrates that the 3D image from LSCM characterizes the structure accurately. This should give us intuitive insight into the complex structure and enables us to determine quantities difficult to obtain from the conventional scattering methods, such as the mean curvature of the interface. This analysis is in progress.

References and Notes

(1) Gunton, J. D.; Miguel, M.; Sahni, P. In *Phase Transitions and Critical Phenomena*; Domb, C., Lebowitz, J. L., Eds.; Academic Press: New York, 1983; p 269.
(2) Binder, K. In *Materials Science and Technology, Vol. 5, Phase Transformation in Materials*; Haasen, P., Ed.; VCH: Weinheim, FRG, 1991.
(3) Hashimoto, T. *Phase Transitions* **1988**, *12*, 47; *Materials Science and Technology, Vol. 12, Structure and Properties of Polymers*; VCH: Weinheim, FRG, 1993.
(4) Nishi, T.; Wang, T. T.; Kwei, T. K. *Macromolecules* **1975**, *18*, 227. Tanaka, H.; Suzuki, T.; Hayashi, T.; Nishi, T. *Macromolecules* **1992**, *25*, 4453. Tanaka, H. *Phys. Rev. Lett.* **1994**, *72*, 1702.
(5) Hashimoto, T.; Itakura, M.; Hasegawa, H. *J. Chem. Phys.* **1986**, *85*, 6118. Hashimoto, T.; Itakura, M.; Shimidzu, N. *J. Chem. Phys.* **1986**, *85*, 6773. Sato, T.; Han, C. C. *J. Chem. Phys.* **1988**, *88*, 2057.
(6) Motowoka, M.; Jinnai, H.; Hashimoto, T.; Qiu, Y.; Han, C. C. *J. Chem. Phys.* **1993**, *99*, 2095. Jinnai, H.; Hasegawa, H.; Hashimoto, T.; Han, C. C. *J. Chem. Phys.* **1994**, *99*, 4845. Jinnai, H.; Hasegawa, H.; Hashimoto, T.; Han, C. C. *J. Chem. Phys.* **1994**, *99*, 8154.
(7) Strobl, G. R. *Macromolecules* **1985**, *18*, 558. Meier, H.; Strobl, G. R. *Macromolecules* **1987**, *20*, 649.
(8) Langer, J. S.; Bar-on, M.; Miller, H. D. *Phys. Rev. A* **1975**, *11*, 1417.
(9) See, for example: Wilson, T. *Confocal Microscopy*; Academic Press: London, 1990.
(10) James, J.; Tanke, H. J. *Biomedical Light Microscopy*; Kluwer Academic Press: Dordrecht, The Netherlands, 1991.
(11) Verhoogt, H.; van Dam, J.; Posthuma de Boer, A.; Draaijer, A.; Houpt, P. M. *Polymer* **1993**, *34*, 1325–1329.
(12) Li, L.; Sosnowski, S.; Chaffey, C. E.; Balke, S. T.; Winnik, M. A. *Langmuir* **1994**, *10*, 2495–2497.
(13) Izumitani, T.; Hashimoto, T. *J. Chem. Phys.* **1985**, *83*, 3694.
(14) Hashimoto, T.; Izumitani, T.; Takenaka, M. *Macromolecules* **1989**, *22*, 2293.
(15) Izumitani, T.; Takenaka, M.; Hashimoto, T. *J. Chem. Phys.* **1990**, *92*, 3213.
(16) Hashimoto, T.; Takenaka, T.; Jinnai, H. *J. Appl. Crystallogr.* **1991**, *24*, 457. Takenaka, M.; Hashimoto, T. *J. Chem. Phys.* **1992**, *96*, 6177.
(17) Chakrabarti, A.; Toral, A.; Gunton, J. D.; Muthukumar, M. *J. Chem. Phys.* **1990**, *92*, 6899. Shinozaki, A.; Oono, Y. *Phys. Rev. Lett.* **1991**, *66*, 173. Koga, T.; Kawasaki, K. *Phys. Rev. A* **1991**, *44*, R817.
(18) Koga, T.; Kawasaki, K. *Physica A* **1993**, *196*, 389. Koga, T.; Kawasaki, K.; Takenaka, M.; Hashimoto, T. *Physica A* **1993**, *198*, 473.
(19) Bates, F. S.; Wiltzius, P. *J. Chem. Phys.* **1989**, *91*, 3258.
(20) Takenaka, M.; Izumitani, T.; Hashimoto, T. *J. Chem. Phys.* **1990**, *92*, 4566.
(21) The upward deviation of the FFT of the LSCM and simulation data from Porod's law, $S(q) \sim q^{-4}$, in the large q-region is due to the discreteness of the data.

MA9502765

CORRECTIONS

R. G. Larson: Simulation of Lamellar Phase Transitions in Block Copolymers. Volume 27, Number 15, July 18, 1994, pp 4198–4203.

The abscissa of Figure 7 is mislabeled; instead of "$\bar{N}$", it should be "$/n(\bar{N})$", the natural logarithm of $\bar{N}$.

MA946303T